Available online at www.sciencedirect.com
ScienceDirect
Journal of Sound and Vibration 306 (2007) 877–889
JOURNAL OF SOUND AND VIBRATION
www.elsevier.com/locate/jsvi

Acoustic radiation from a laminated composite plate reinforced by doubly periodic parallel stiffeners

X.W. Yin[a,*], X.J. Gu[a], H.F. Cui[b], R.Y. Shen[a]

[a]*State Key Laboratory of Mechanical System and Vibration, Shanghai Jiao Tong University, Shanghai 200240, China*
[b]*Wuxi Institute of Technology, Wuxi, Jiangsu 214073, China*

Received 2 September 2006; received in revised form 2 June 2007; accepted 30 June 2007

Abstract

Acoustic radiation from a point-driven, infinite fluid-loaded, laminated composite plate which is reinforced by doubly periodic parallel stiffeners is investigated theoretically. The stiffeners interact with the plate only through normal forces. Fourier transform is used for solving the responses of the plate, and the stationary phase approximate is then employed to find an expression for the far field pressure. Acoustic radiation from a stiffened uniform plate composed of multiple isotropic layers is calculated with the present stiffened, laminated composite plate theory, and with the stiffened uniform isotropic plate theory that Mace has proposed. Comparison of the numerical results reveals the validity of our work. Characteristics of the acoustic radiation from a stiffened laminated composite plate are examined through examples and some physical interpretations of significant features are also offered.

1. Introduction

Laminated composite plates are extensively used in many engineering applications due to their excellent properties with lower weight and higher strength and stiffness than most metallic materials, which are often reinforced by stiffening members such as frames or ribs. So the problem of the acoustic radiation from stiffened laminated composite plates is of great concern in many related fields. For laminated plates, they are usually modeled as a two-dimensional problem, i.e., an equivalent single layer, so the fully developed uniform isotropic plate theories [1,2] can be conveniently extended to the laminated plate theories [3,4], which are based either on the Kichhoff hypothesis or on the shear deformation assumptions. Among them, the classical laminated plate theory (CLPT) is based on the Kirchhoff–Love kinematic hypothesis which states that straight lines normal to the undeformed midplane remain straight and normal to the midplane after deformation (i.e., the transverse shear strain are neglected). However, it is inadequate because it underestimates the deflections and overestimates resonant frequencies and buckling loads, so it has to be restricted to the case of thin plate.

More accurate results are provided by first-order shear deformation theory [5,6] (FSDT) or other higher-order shear deformation theories [7,8] (HSDT). First-order shear deformation theory is based on

*Corresponding author.
E-mail address: x.w.yin@sjtu.edu.cn (X.W. Yin).

0022-460X/$ - see front matter © 2007 Elsevier Ltd. All rights reserved.
doi:10.1016/j.jsv.2007.06.047

Reissner–Mindlin-type assumptions which take into account the transverse shear deformation, however, it requires shear correction factors to compensate for the errors resulting from the approximation of the nonlinear shear-strain distribution by the linear distribution. More refined theories such as second and higher-order plate theories, which use higher-order polynomials in the expansions of the displacement components through the thickness of the plate, are proposed by Reddy and his associates [7–9] for laminated plates and shells.

When plates are reinforced by stiffening members, their dynamic characteristics are quite different from those of the uniform plates. The dynamic analysis of the stiffened plates has been extensively conducted by numerous researchers. The effects of the stiffening members play an important role in the vibration and acoustic radiation from a stiffened plate. Maidanik [10] showed that the rigid periodic line supports attached to an infinite plate increase the acoustic radiation efficiency at frequencies below the critical frequency. Maidanik [11] and Crighton and Maidanik [12] concluded a physical interpretation on the effects of the stiffeners that the stiffening members may convert high, nonradiating, subsonic wavenumbers into low, radiating, supersonic wavenumbers.

Two main categories for the theories of plates reinforced with periodic stiffeners, one of which is Mace's wavenumber transform method [13], the other is Mead's space harmonic wave theory [14,15], and the former was also considered as an implicit form of the latter in mathematical formulation. Mace investigated the acoustic radiation from an infinite uniform plate with parallel or orthogonal periodic stiffeners which can convert free waves at a certain wavenumber into infinite free waves with periodic wavenumber components. This was confirmed by Burroughs [16] in the case of a cylindrical shell with doubly periodic rings. Space harmonic series was employed by Rumerman [17] for the wave propagation and vibration of a ribbed thin plate, in which the forces and moments due to the stiffeners are described in forms of line transfer impedances. Finite plates reinforced by stiffeners were also the interests of the investigators. Keltie [18] gave the acoustic response of a finite fluid-loaded thin plate with arbitrary attached stiffeners, in which the ribs were modeled as simple inertial reactions providing transverse forces to the plate, and the vibration of the plates is taken as the expansion of the in *vacuo* modes.

Little attention [15,19,20] was paid to the vibration and acoustic radiation from a laminated, or even composite plate with periodic stiffeners. In the present paper, the vibration and acoustic radiation from a laminated plate reinforced by doubly periodic parallel stiffeners is investigated by using Mace's method for an infinite uniform isotropic plate. The problem is based on the classical laminated composite plate theory, the Helmholtz wave equation, and boundary conditions at the fluid-plate interface and at infinity. The solution is obtained by using Fourier transform, and the stationary phase approximation is used to find an expression for the far field acoustic pressure. Far field radiation from an isotropic plate with doubly periodic stiffeners is calculated with classical laminated composite plate theory and with thin isotropic plate theory proposed by Mace, respectively. Comparison of the numerical results reveals the validity of our work. Further numerical results are represented for discussion of the characteristics of vibration and acoustic response for stiffened laminated plates.

2. Description of mathematical model

An infinite, laminated composite plate rests on the plane $z = 0$ with acoustic fluid occupying the half-space $z > 0$ as shown in Fig. 1. Two sets of parallel frames are attached to the lower plane of the plate in x direction. The first set of frames are the smaller frames with a spacing l and the second set of the frames, namely, bulkheads, are the larger frames that replace every qth frame in the smaller set. Thus, the spacing of the second set of frames is ql. The origin of the plate's coordinates may be selected at one point in the plate's midplane, and which is also with a distance of x_0 to one arbitrary bulkhead in x direction. Thus, the terms in the expressions of the forces due to the frames and the bulkheads shall be defined as $\delta(x - x_0 - nl)$ and $\delta(x - x_0 - nql)$, respectively. As an algebraic convenience, x_0 will be set zero. Since the thickness of the plate is sufficiently thin with comparison to its other two dimensions, the interfaces between the plate and the fluid, as well as the intersections between the plate and the frames, are chosen from the plane $z = 0$. The plate is driven by an external transverse force p_e which is located at (x_0, y_0) and with an amplitude of Q. For problems of harmonic vibration, all of the loadings have a time dependence $e^{i\omega t}$, where ω is the circular frequency and $e^{i\omega t}$ will henceforth be suppressed throughout.

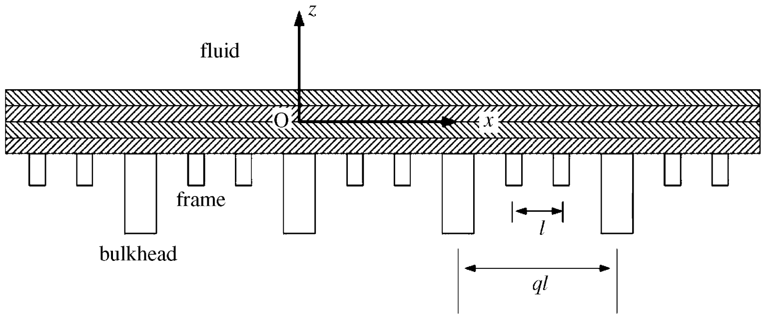

Fig. 1. An infinite laminated composite plate with doubly periodic parallel stiffeners.

The classical Kirchhoff–Love thin plate theory is conveniently extended to laminated plates by applying the appropriate integration through lamina, and stress–strain relations based on the following complementary assumptions:

(1) The layers are perfectly bonded together.
(2) The material of each layer is linearly elastic.
(3) The material has two planes of material symmetry (orthotropic).

With the above assumptions, the motions of a fluid-loaded, laminated composite plate with doubly periodic parallel stiffeners are expressed in the following matrix form [21]:

$$\begin{bmatrix} L_{11} & L_{12} & L_{13} \\ L_{21} & L_{22} & L_{23} \\ L_{31} & L_{32} & L_{33} \end{bmatrix} \begin{Bmatrix} u_0 \\ v_0 \\ w \end{Bmatrix} = \begin{Bmatrix} 0 \\ 0 \\ \left[p_e - p_a(x,y,0) - p_f(x,y) - p_b(x,y)\right] \end{Bmatrix}, \tag{1}$$

where u_0,v_0 are the membrane displacements in the plate's middle plane, w is the transverse displacement of the plate. $p_a(x,y,z)$, $p_e = Q\delta(x-x_0)\delta(y-y_0)$ are the acoustic pressure in the fluid and the point driven force on (x_0,y_0), respectively. $p_f(x,y)$, $p_b(x,y)$ are the reactive forces due to the two sets of stiffeners. L_{ij} $(i = 1,3; j = 1,3)$ are differential operators for a thin laminated composite plate, which will be given in Appendix A.

Eq. (1) can be easily solved by Fourier transformation with the following transform pair:

$$\tilde{w}(\alpha,\beta) = \int_{-\infty}^{+\infty}\int_{-\infty}^{+\infty} w(x,y)\mathrm{e}^{\mathrm{i}(\alpha x+\beta y)}\,\mathrm{d}x\,\mathrm{d}y, \tag{2}$$

$$w(x,y) = \frac{1}{4\pi^2}\int_{-\infty}^{+\infty}\int_{-\infty}^{+\infty} \tilde{w}(\alpha,\beta)\mathrm{e}^{-\mathrm{i}(\alpha x+\beta y)}\mathrm{d}\,\alpha\,\mathrm{d}\beta. \tag{3}$$

Transforming Eq. (1), gives

$$\begin{bmatrix} \tilde{L}_{11} & \tilde{L}_{12} & \tilde{L}_{13} \\ \tilde{L}_{21} & \tilde{L}_{22} & \tilde{L}_{23} \\ \tilde{L}_{31} & \tilde{L}_{32} & \tilde{L}_{33} \end{bmatrix} \begin{Bmatrix} \tilde{u}_0 \\ \tilde{v}_0 \\ \tilde{w} \end{Bmatrix} = \begin{Bmatrix} 0 \\ 0 \\ \left[\tilde{p}_e - \tilde{p}_a - \tilde{p}_f - \tilde{p}_b\right] \end{Bmatrix}, \tag{4}$$

where $\tilde{L}_{ij}$ $(i = 1,3; j = 1,3)$ are the transformed operators for a thin laminated composite plate, which will be given in Appendix B. Before the solving of Eq. (4), it is found that the terms $\tilde{p}_a$, $\tilde{p}_b$ and $\tilde{p}_f$ in the right-hand side of Eq. (4) are functions of transformed transverse displacement $\tilde{w}$, so they shall be transposed to the left-hand side and appended to their counterpart, i.e., the term $\tilde{L}_{33}\tilde{w}$. However, due to the presence of periodic frames, $\tilde{p}_b$ and $\tilde{p}_f$ involve transformed transverse displacement with infinite, converted wavenumber components in terms of $\tilde{w}(\alpha - 2n\pi/l, \beta)$, which makes the above idea come true with great difficulties. In the present paper, Eq. (4) is solved in the classical concept of stiffness as did by Mace and Burroughs. When all the loadings are beforehand assumed to be independent of the plate's displacements, the transformed transverse displacement $\tilde{w}(\alpha,\beta)$ in the wavenumber space is given as follows by solving Eq. (4):

$$\tilde{w}(\alpha,\beta) = [\tilde{p}_e - \tilde{p}_a - \tilde{p}_f - \tilde{p}_b]\det\left(\begin{bmatrix} \tilde{L}_{11} & \tilde{L}_{12} \\ \tilde{L}_{21} & \tilde{L}_{22} \end{bmatrix}\right) \Big/ \det(\tilde{L}). \tag{5}$$

Eq. (5) can be rewritten in the following form

$$\tilde{K}_s(\alpha,\beta)\tilde{w}(\alpha,\beta) = \tilde{p}_e - \tilde{p}_a - \tilde{p}_f - \tilde{p}_b, \tag{6}$$

where $\tilde{K}_s$ is the transformed spectral stiffness and can be given as follows:

$$\tilde{K}_s(\alpha,\beta) = \left(\det\left(\begin{bmatrix} \tilde{L}_{11} & \tilde{L}_{12} \\ \tilde{L}_{21} & \tilde{L}_{22} \end{bmatrix}\right) \Big/ \det(\tilde{L})\right)^{-1}. \tag{7}$$

When we examine the elements $\tilde{L}_{ij}$ in Eq. (7) through the laminated composite plate theory (a more brief outline is given in Appendix A and B), the transverse motion of a laminated composite plate includes the contribution of the in-plane motions due to not only the Poisson effect, but also the particular feature of the laminated plate, i.e., bending–extension coupling, which make the characteristics of the vibration and acoustic radiation from a laminated composite plate more complex than those from a uniform isotropic plate.

For sake of the integrity of this paper, the work done by Mace [13] as well as Burroughs [16] will be frequently cited and henceforth will not be labeled as citations.

2.1. The fluidloading

The acoustic pressure in the half-infinite space above $z>0$ satisfies the Helmholtz equation

$$\left(\frac{\partial^2}{\partial x^2} + \frac{\partial^2}{\partial y^2} + \frac{\partial^2}{\partial z^2}\right)p_a + \left(\frac{\omega^2}{c_0^2}\right)p_a = 0, \tag{8}$$

where c_0 is the speed of sound in the fluid. The coupling between the plate and the fluid satisfies the momentum equation in z-axis as

$$\frac{\partial p_a}{\partial z}|_{z=0} = \omega^2 \rho_0 w, \tag{9}$$

where ρ_0 is the density of the fluid . Taking the Fourier transform of Eqs. (8) and (9), yields

$$\tilde{p}_a(\alpha,\beta,0) = -\omega^2\rho_0\tilde{w}(\alpha,\beta)/\gamma(\alpha,\beta), \tag{10}$$

where

$$\gamma^2 = \alpha^2 + \beta^2 - \omega^2/c_0^2 \tag{11}$$

and γ is to be evaluated such that: $\mathrm{Re}(\gamma)\geqslant 0$, $\mathrm{Im}(\gamma)\geqslant 0$ if $\mathrm{Re}(\gamma)=0$, in order that the radiation conditions for outgoing waves are met.

2.2. Reactive froces by stiffeners

The equation of motion of the nth frame, which is modeled as a Bernoulli–Euler beam excited by a line force $F_n(y)$ along the line $x = nl$ is

$$E_f I_f \frac{\mathrm{d}^4 u_n}{\mathrm{d}y^4} - \rho_f A_f \omega^2 u_n = F_n, \tag{12}$$

where $E_f I_f$ and $\rho_f A_f$ are the bending stiffness and mass per unit length of the frame and $u_n(y)$ is the frame displacement. The sum of the forces acting on the plate due to the frames is therefore

$$p_f(x,y) = \sum_{n=-\infty}^{n=+\infty}\left(E_f I_f \frac{\mathrm{d}^4 u_n}{\mathrm{d}y^4} - \rho_f A_f \omega^2 u_n\right)\delta(x - nl). \tag{13}$$

The transform of these reactive forces is

$$\tilde{p}_f(\alpha,\beta) = \left(E_f I_f \beta^4 - \rho_f A_f \omega^2\right) \sum_{n=-\infty}^{+\infty} \tilde{u}_n(\beta) e^{i\alpha n l}. \tag{14}$$

Since the transverse displacements of the frame and the plate are equal at $x = nl$, we have

$$u_n(y) = w(nl, y), \tilde{u}_n(\beta) = w(nl, \beta). \tag{15}$$

By definition

$$w(nl,\beta) = \frac{1}{2\pi}\int_{-\infty}^{\infty} \tilde{w}(\alpha^*,\beta) e^{-i(\alpha^* nl)}\, d\alpha^* \tag{16}$$

and therefore

$$\sum_{n=-\infty}^{\infty} \tilde{u}_n(\beta) e^{i\alpha nl} = \frac{1}{2\pi}\sum_{n=-\infty}^{\infty}\int_{-\infty}^{\infty} \tilde{w}(\alpha^*,\beta) e^{i(\alpha-\alpha^*)nl}\, d\alpha^*. \tag{17}$$

The Poisson sum formula can be used to show that

$$\sum_{n=-\infty}^{\infty} e^{i\alpha nl} = 2\pi \sum_{n=-\infty}^{\infty} \delta(\alpha l - 2n\pi) \tag{18}$$

and thus

$$\sum_{n=-\infty}^{\infty} \tilde{u}_n(\beta) e^{i\alpha nl} = \sum_{n=-\infty}^{\infty}\int_{-\infty}^{\infty} \tilde{w}(\alpha^*,\beta)\delta((\alpha-\alpha^*)l - 2n\pi) d\alpha^* = \frac{1}{l}\sum_{n=-\infty}^{\infty} \tilde{w}\left(\alpha - \frac{2n\pi}{l}, \beta\right). \tag{19}$$

The transform of the frame reactions is finally given by

$$\tilde{p}_f(\alpha,\beta) = \left(\frac{K_f}{l}\right)\sum_{n=-\infty}^{n=+\infty} \tilde{w}(\alpha - 2n\pi/l, \beta), \tag{20}$$

where

$$K_f = E_f I_f \beta^4 - \rho_f A_f \omega^2. \tag{21}$$

A similar expression can be found for the reactive forces due to the bulkheads, which lie along the lines $x = nql$. However, in the derivation above a frame was assumed to lie at $x = nl$ for all integers n. The stiffness of a frame must therefore be subtracted from the stiffness of each bulkhead. Thus

$$\tilde{p}_b(\alpha,\beta) = \left(\frac{(K_b - K_f)}{ql}\right)\sum_{n=-\infty}^{n=+\infty} \tilde{w}(\alpha - 2n\pi/l, \beta), \tag{22}$$

where

$$K_b = E_b I_b \beta^4 - \rho_b A_b \omega^2. \tag{23}$$

3. Solutions of transformed equations

Substituting Eqs. (10), (20) and (22) into Eq. (6) yields Mace's solution which is written as follows:

$$\tilde{w}(\alpha,\beta) = \frac{\tilde{p}_e}{S(\alpha,\beta)} - \frac{(K_b - K_f)}{S(\alpha,\beta)ql}\sum_{n=-\infty}^{\infty} \tilde{w}\left(\alpha - \frac{2n\pi}{ql}, \beta\right) - \frac{K_f}{S(\alpha,\beta)l}\sum_{n=-\infty}^{\infty} \tilde{w}\left(\alpha - \frac{2n\pi}{l}, \beta\right), \tag{24}$$

where

$$S(\alpha,\beta) = \tilde{Z}s(\alpha,\beta) - \rho_0\omega^2/\gamma, \tag{25}$$

is the spectral dynamic stiffness of the fluid-loaded, laminated composite plate. Mace has given the solution to Eq. (24) as

$$\tilde{w}(\alpha) = F(\alpha) - \left\{ GP_0(\alpha) + \frac{H\sum_{r=0}^{q-1} P_r(\alpha)/1 + GY_r(\alpha)}{\left\{1 + H\sum_{r=0}^{q-1} Y_r(\alpha)/1 + GY_r(\alpha)\right\}} \right\} \Bigg/ \{S(\alpha) \times (1 + GY_0(\alpha))\} \tag{26}$$

with the following definitions

$$F(\alpha) = \tilde{p}_e/S,\ G = K_f/l,\ H = (K_b - K_f)/ql,\ e = 2\pi/l \tag{27}$$

$$P_r(\alpha) = \sum_{m=-\infty}^{\infty} F\left(\alpha - \frac{\mathrm{er}}{q} - \mathrm{em}\right),\ Y_r(\alpha) = \sum_{m=-\infty}^{\infty} 1/S\left(\alpha - \frac{\mathrm{er}}{q} - \mathrm{em}\right). \tag{28}$$

The far field acoustic radiation in spherical coordinates (R,θ,ϕ) can be given with the application of one standard procedure, i.e., stationary phase approximation

$$P(R, \theta, \phi) = -\rho_0\omega^2\tilde{w}(\alpha_0, \beta_0)\mathrm{e}^{-\mathrm{i}k_0R}/2\pi R, \tag{29}$$

where the stationary point is defined as follows

$$\alpha_0 = (\omega/c_0)\sin\theta\cos\phi, \beta_0 = (\omega/c_0)\sin\theta\sin\phi, \tag{30}$$

and R is the distance from the field point to the origin. It is clear from Eq. (29) that the far field pressure at an observation point (R,θ,ϕ) only involves contribution from transformed displacement at a single wavenumber pair (α_0,β_0) which is specified by Eq. (30), and the contribution from all other wavenumbers may be filtered out due to the rapidly oscillatory integral in the expression for the far field. By the way, it will be noted that the origin of the spherical coordinates shall be coincident with the origin of the plate's coordinates, besides, the θ and ϕ axes shall be orientated along x and z axes for the plate's coordinates, respectively.

4. Numerical results

In this section, numerical results based on Eq. (29) are calculated for the far field (R = 50.0 m, $\theta = \phi = 45°$) acoustic radiation from a point driven, laminated composite plate reinforced with doubly periodic parallel stiffeners. For all the numerical examples, the external force is located at (1.0 m, 0.0 m) and with an amplitude of 1.0 N. The sound pressure levels in Figs. (2)–(8) are normalized with reference to 1 μP_a pressure, and corrected to the field point ($R_0 = 1.0$ m, $\theta_0 = \phi_0 = 45°$). This is because the sound pressure in the near field is unsteady, the aforementioned procedure is standard, and extensively used to describe the acoustic field from an underwater elastic structure.

At first, to validate our work, a doubly stiffened uniform isotropic plate, whose parameters are given in S.I. units as shown in Table 1, is considered to be a laminated plate with three uniform isotropic layers. Therefore, numerical results for the acoustic radiation from a stiffened uniform isotropic plate are represented with three plate theories: classical thin plate theory that was used by Mace, Timoshenko-Mindlin thick plate theory and classical laminated composite plate theory.

Numerical results are shown in Fig. 2 for a plate without bulkheads and in Fig. 3 for a plate with bulkheads. From Figs. 2 and 3, the results from the laminated composite plate theory agree well with those from thin plate theory used by Mace except at high frequency range, therefore, our theory for acoustic radiation from a laminated composite plate reinforced with doubly periodic parallel stiffeners is partly verified. Moreover, with comparison to the Timoshenko-Mindlin thick plate theory, the classical thin plate theory shall provide good accuracy for dynamics of a plate in low and medium frequency ranges, which means that the effects of rotatory inertia and transverse shear may come into effect only at very high frequencies, i.e. when the plate thickness exceeds $\lambda_s/20$ as concluded by Junger and Feit [22], where λ_s is the wavelengths of free shear waves in the plate.

Numerical results for a laminated plate with and without the bulkheads are shown in Fig. 4. When the laminated plate is only reinforced by the first set of more closely spaced stiffeners, the first peak in the

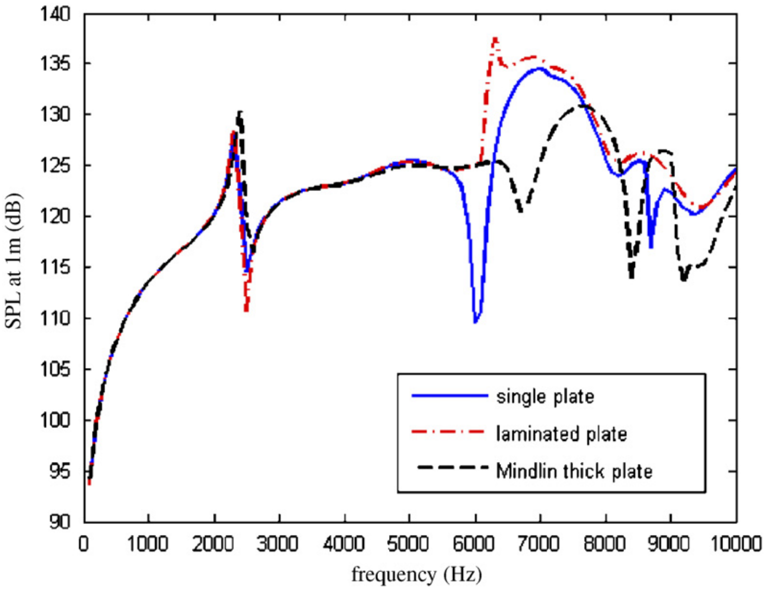

Fig. 2. Comparison between three plate theories (without bulkheads).

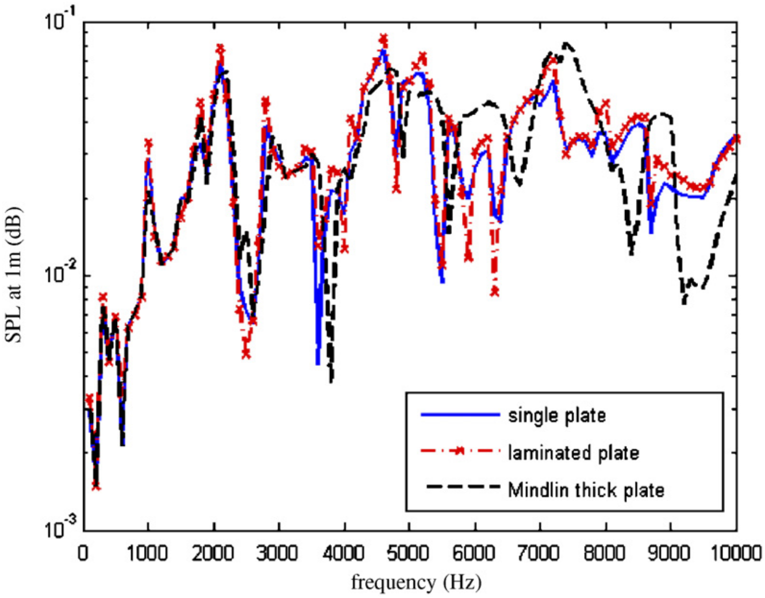

Fig. 3. Comparison between three plate theories (with bulkheads).

sound pressure level occurs near 2300 Hz. And when the second set of more widely spaced stiffeners (bulkheads) are added, a series of additional peaks occur at lower frequencies below 2300 Hz, as well as at higher frequency ranges. This phenomena was first observed by Mace for a stiffened uniform isotropic plate, and then by Burroughs for a ring-reinforced cylindrical shell, where the wavenumber conversion mechanism due to the presence of periodic stiffening members was discovered, however, they both ignored that the wavenumber conversion, which is due to the second set of more widely spaced stiffeners, can also make contribution to the additional acoustic radiation peaks at higher frequency ranges. With inspection of Eqs. (20) and (22), the presence of periodic stiffeners possess a bidirectional wavenumber conversion mechanism, namely, it can convert not only high wavenumber components into low

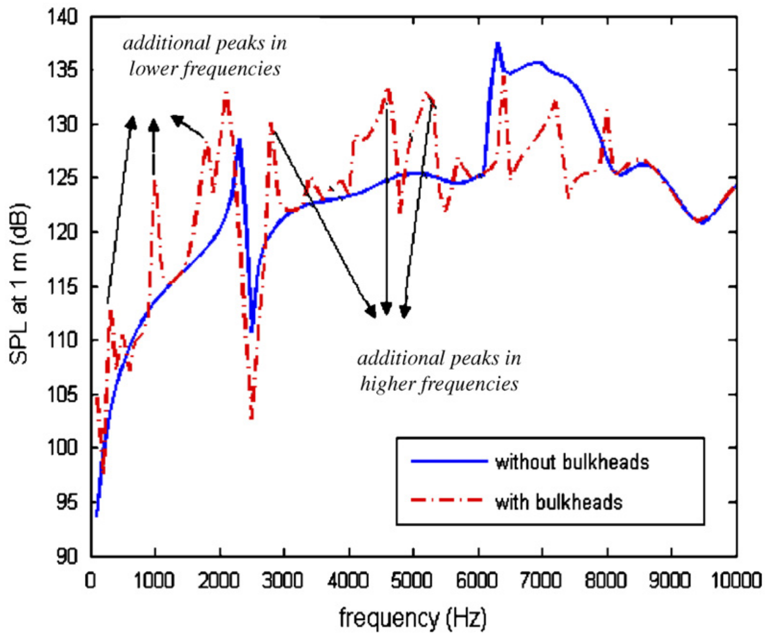

Fig. 4. Effects of bulkheads on far field sound pressure level.

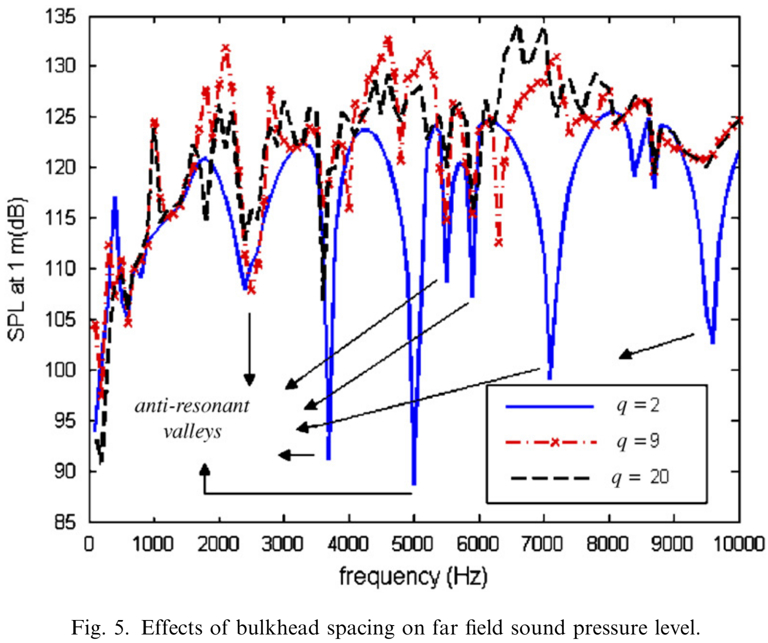

Fig. 5. Effects of bulkhead spacing on far field sound pressure level.

wavenumber components (when $n>0$), but also low wavenumber components into high wavenumber components (when $n<0$).

The effect of bulkhead spacing on acoustic radiation is represented in Fig. 5. If the bulkhead spacing ql is close to the frame spacing l, for example, when $q=2$, very deep anti-resonant valleys are observed and they play an absolutely dominant role in the acoustic radiation at the anti-resonant frequencies, which display a distinctively different feature from that with larger bulkhead spacing, i.e., $q=9$, $q=20$. A sufficiently reasonable interpretation can not be offered in the present paper and further investigations are

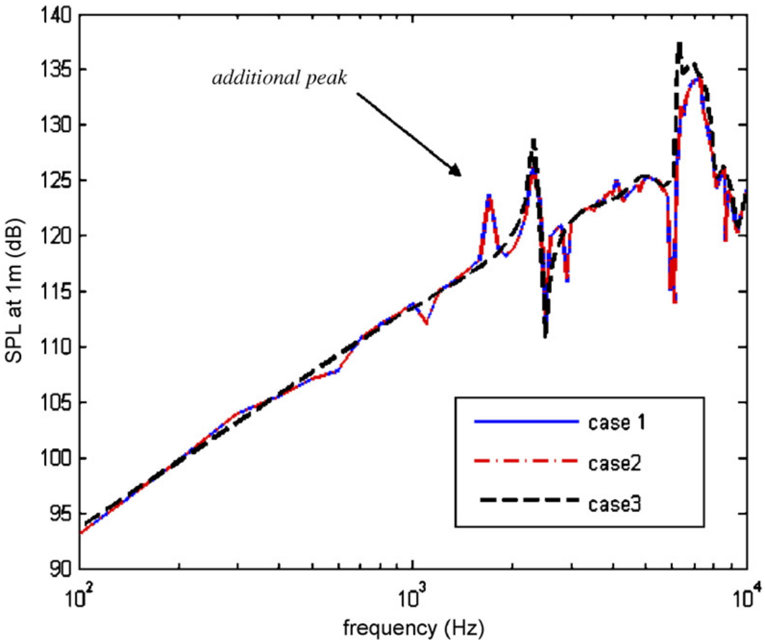

Fig. 6. Effects of the middle layer's stiffness on far field sound pressure level.

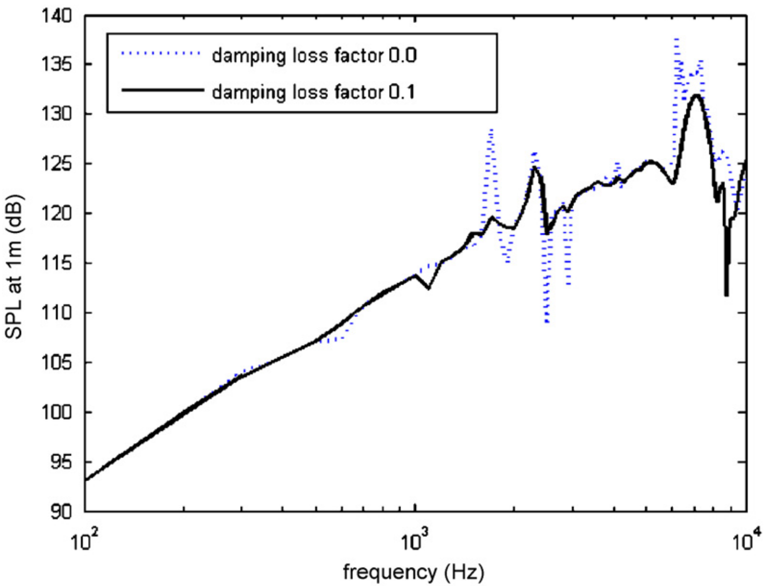

Fig. 7. Effects of plate damping loss factor on far field sound pressure level.

therefore necessary for better understanding this feature. Nevertheless, we are reminded that proper design of bulkhead spacing may effectively control the acoustic radiation from a structure with doubly periodic stiffeners.

In engineering applications, laminated composite plates are usually constituted with many plies, each of whose material property axes may be oriented along different directions. Constrained layer damping (CLD) is one of the special cases, in which the middle layer is frequently assumed to undergo only pure shear [15]. The effects of the middle layer stiffness on acoustic radiation were seldom considered. In this section,

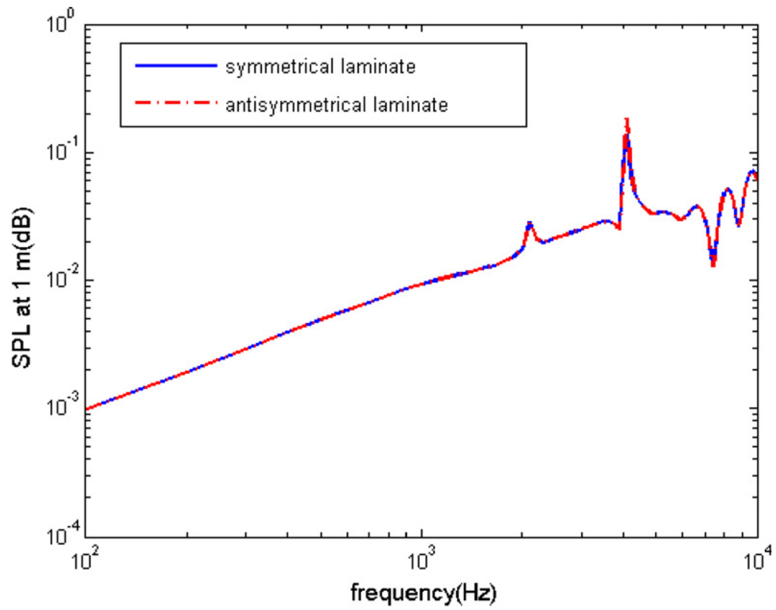

Fig. 8. Comparison between sound pressure levels for a stiffened symmetrical laminate and a stiffened antisymmetrical laminate.

Table 1
Parameters of the fluid-loaded, laminated composite plate

Density of plate	ρ	7800	Density of frames	ρ_f	7800
Young's modulus	E	2.0×10^{11}	Inertia moment	I_f	6.66×10^{-7}
Poisson's ratio	v	0.3	Section area	A_f	2.58×10^{-4}
Loss factor	η	0.02	Density of bulkheads	ρ_b	7800
Fluid density	ρ_0	1000	Inertia moment	I_b	1.6×10^{-4}
Sound speed	c_0	1450	Section area	A_b	4.0×10^{-4}
Plate thickness	h	0.003×3	Spacing	$q=9$	$l=0.1524$

Table 2
Main parameters of the stiffened, three-layered sandwich plate

	E_x and E_y of the middle layer	E_x and E_y of the lower and upper layers	Density of each layer	Thickness	Stiffened only by
Case 1	2.0×10^{5}	2.0×10^{11}	7800	0.003×3	The first set of frames in Table 1.
Case 2	2.0×10^{8}	2.0×10^{11}	7800	0.003×3	
Case 3	2.0×10^{11}	2.0×10^{11}	7800	0.003×3	

a three-layered sandwich plate with different Young's modulus of middle layer is investigated to evaluate such effects. The main parameters of the stiffened, laminated plate are listed in Table 2, and the other parameters are the same as those in Table 1.

In Fig. 6, the effect of the middle layer's stiffness on acoustic radiation is represented in three cases. Reduction of Young's modulus of the middle layer produces one additional resonant peak as shown through the curves corresponding to cases 1 and 2. This is because the middle layer in case 1, as well in case 2, is very soft with comparison to that in case 3, each of their surface layers may vibrate effectively at a visible lower resonant frequency, and thus its vibration makes contribution to the acoustic field. In plate theories, material layer close to the midplane is not effective for providing bending stiffness, so this

Table 3
Parameters of the stiffened symmetrical/antisymmetrical laminate

Layer no.	E_x	E_y	v_{xy}	v_{yx}	Damping	Density	Layer thickness	Ply angle (deg.)	Stiffened only by
1	3.0×10^{10}	3.0×10^{11}	0.03	0.3	0.02	7800	0.0015	75	The first set of frames in Table 1.
2	2.0×10^{10}	2.0×10^{11}	0.03	0.3	0.02	7800	0.0015	60	
3	1.0×10^{10}	1.0×10^{11}	0.03	0.3	0.02	7800	0.0015	45	
4	1.0×10^{10}	1.0×10^{11}	0.03	0.3	0.02	7800	0.0015	±45	
5	2.0×10^{10}	2.0×10^{11}	0.03	0.3	0.02	7800	0.0015	±60	
6	3.0×10^{10}	3.0×10^{11}	0.03	0.3	0.02	7800	0.0015	±75	

contribution is very limited, and the acoustic radiation is not sensitive to the change of stiffness in the middle layer.

The effect of structural damping on the acoustic radiation is illustrated in Fig. 7. According to the time dependence $e^{i\omega t}$, the complex modulus of elasticity may take the form of $E(1+i\eta)$, where η is the damping loss factor. Adding damping reduces both the peaks and valleys in the numerical results shown in Fig. 7, but has little impact at frequencies where peaks or valleys do not occur.

One of the most remarkable features of a laminated composite plate is that the plate is a combination of many composite layers with different lamination schemes. For example, when ply stacking sequence, material, and geometry are symmetrical with the midplane of the laminate, the laminate is called a symmetrical laminate. Similarly is defined the antisymmetrical laminate. For symmetrical laminates, the coupling between bending and extension will be eliminated, i.e., the coupling stiffenesses B_{ij} (see Appendix A and B) are zero, while for antisymmetrical laminates, the coupling stiffenesses B_{ij} are not zero. The effects of these features on acoustic radiation from a stiffened, laminated composite plate are of great significance.

In this section, as listed in Table 3, a symmetrical laminate (all ply angles are positive) and an antisymmetrical laminate (ply angles for layers 1–3 are positive, for layers 4–6 are negative) are considered as examples for evaluating the coupling effects on far field acoustic radiation. Numerical results for the acoustic radiation are presented in Fig. 8 for the stiffened symmetrical laminate and the stiffened antisymmetrical laminate, and there is almost no difference between them. Since the applied force is not in-plane but transverse, the bending motions in the symmetrical and the antisymmetrical laminates are so dominant that the coupling stiffenesses B_{ij} due to different angle-ply schemes in the above two cases play a relatively minor role in the acoustic radiation.

5. Conclusions

An equation is derived for acoustic radiation from a point-driven, fluid-loaded, laminated composite plate reinforced by doubly periodic stiffeners, which is an extension of mace's work for an isotropic plate with doubly periodic stiffeners. Our work is verified through an example of a stiffened uniform isotropic plate, the acoustic radiation from which is calculated with application of the present method and Mace's method, respectively.

Through numerical results, it is shown that the wavenumber conversion mechanism due to the presence of stiffeners is a bidirectional one, which is an improved version of Mace and Burroughs' discovery. A series of very deep anti-resonant valleys for sound pressure level are observed when the spacing of the bulkheads is close to that of the first set of stiffeners, and they play an absolutely dominant role in the acoustic radiation at the anti-resonant frequencies, which display a distinctively different feature from that with larger bulkhead spacing.

Structural damping can only reduce the valleys and peaks in acoustic radiation, while the middle layer stiffness has little impact on the acoustic radiation. When the external point force is transverse, the lamination schemes of symmetrical and antisymmetrical laminate play a minor role in the acoustic radiation.

Appendix A

The differential operators L_{ij} in Eq. (1) are symmetric and listed in the following

$$L_{11} = A_{11}\frac{\partial^2}{\partial x^2} + 2A_{16}\frac{\partial^2}{\partial x \partial y} + A_{66}\frac{\partial^2}{\partial y^2} + m\omega^2, \quad \text{(A.1)}$$

$$L_{12} = A_{16}\frac{\partial^2}{\partial x^2} + (A_{12} + A_{66})\frac{\partial^2}{\partial x \partial y} + A_{26}\frac{\partial^2}{\partial y^2}, \quad \text{(A.2)}$$

$$L_{22} = A_{66}\frac{\partial^2}{\partial x^2} + 2A_{26}\frac{\partial^2}{\partial x \partial y} + A_{22}\frac{\partial^2}{\partial y^2} + m\omega^2, \quad \text{(A.3)}$$

$$L_{33} = D_{11}\frac{\partial^4}{\partial x^4} + 4D_{16}\frac{\partial^4}{\partial x^3 \partial y} + 2(D_{12} + 2D_{66})\frac{\partial^4}{\partial x^2 \partial y^2} + 4D_{26}\frac{\partial^4}{\partial x \partial y^3} + D_{22}\frac{\partial^4}{\partial y^4} - m\omega^2, \quad \text{(A.4)}$$

$$L_{13} = -B_{11}\frac{\partial^3}{\partial x^3} - 3B_{16}\frac{\partial^3}{\partial x^2 \partial y} - (B_{12} + 2B_{66})\frac{\partial^3}{\partial x \partial y^2} - B_{26}\frac{\partial^3}{\partial y^3}, \quad \text{(A.5)}$$

$$L_{23} = -B_{16}\frac{\partial^3}{\partial x^3} - (B_{12} + 2B_{66})\frac{\partial^4}{\partial x^2 \partial y^2} - 3B_{26}\frac{\partial^3}{\partial x \partial y^2} - B_{22}\frac{\partial^3}{\partial y^3}, \quad \text{(A.6)}$$

where A_{ij} are called extensional stiffnesses, D_{ij} the bending stiffnesses, B_{ij} the bending-extensional coupling stiffnesses, which are defined in terms of the lamina stiffnesses $\bar{Q}_{ij}$ as [21]

$$A_{ij} = \sum_{k=1}^{N} \bar{Q}_{ij}^{(k)}(\varsigma_{k+1} - \varsigma_k), \quad \text{(A.7)}$$

$$B_{ij} = \frac{1}{2}\sum_{k=1}^{N} \bar{Q}_{ij}^{(k)}(\varsigma_{k+1}^2 - \varsigma_k^2), \quad \text{(A.8)}$$

$$D_{ij} = \frac{1}{3}\sum_{k=1}^{N} \bar{Q}_{ij}^{(k)}(\varsigma_{k+1}^3 - \varsigma_k^3), \quad \text{(A.9)}$$

where $\bar{Q}_{ij}^{(k)}$ are known in terms of the engineering constants of the kth layer, namely, Young's modulus, and Poisson ratio, and ς_k is the distance from the midplane to the surface of the kth layer having the furthest z-coordinate. m is the mass per unit area of the plate and $m = \sum_{k=1}^{N} \rho_k h_k$ (N is the number of total layers of the laminated plate).

Appendix B

The transformed operators $\tilde{L}_{ij}$ in Eq. (4) are symmetric and listed in the following

$$\tilde{L}_{11} = -A_{11}\alpha^2 - 2A_{16}\alpha\beta - A_{66}\beta^2 + m\omega^2, \quad \text{(B.1)}$$

$$\tilde{L}_{12} = -A_{16}\alpha^2 - (A_{12} + A_{66})\alpha\beta - A_{26}\beta^2, \quad \text{(B.2)}$$

$$\tilde{L}_{22} = -A_{66}\alpha^2 - 2A_{26}\alpha\beta - A_{22}\beta^2 + m\omega^2, \quad \text{(B.3)}$$

$$\tilde{L}_{33} = D_{11}\alpha^4 + 4D_{16}\alpha^3\beta + 2(D_{12} + 2D_{66})\alpha^2\beta^2 + 4D_{26}\alpha\beta^3 + D_{22}\beta^4 - m\omega^2, \quad \text{(B.4)}$$

$$\tilde{L}_{13} = -iB_{11}\alpha^3 - 3iB_{16}\alpha^2\beta - i(B_{12} + 2B_{66})\alpha\beta^2 - iB_{26}\beta^3, \tag{B.5}$$

$$\tilde{L}_{23} = -iB_{16}\alpha^3 - (B_{12} + 2B_{66})\alpha^2\beta^2 - 3iB_{26}\alpha\beta^2 - iB_{22}\beta^3. \tag{B.6}$$

References

[1] S.P. Timoshenko, K.S. Woinowsky, *Theory of plates and shells*, McGraw Hill, New York, 1959.

[2] R. Szilard, *Theory and analysis of plates (classical and numerical methods)*, Pretice-Hall, New Jersey, 1974.

[3] E. Reissner, Y. Stavsky, Bending and stretching of certain types of heterogeneous aelotropic elastic plates, *ASME Journal of applied mechanics* (1961) 28402–28408.

[4] J.M. Whitney, *Structural analysis of laminated anisotropic plates*, Technomic, Lancaster, 1987.

[5] R.D. Mindlin, Influence of rotatory inertia and shear on flexural motions of isotropic, elastic plates, *ASME Journal of applied mechanics* (1951) 1831–1838.

[6] E. Reissner, On the theory of bending of elastic plates, *Journal of mechanical physics* 1 (1944) 23184–23191.

[7] S.J. Lee, J.N. Reddy, Smart materials and structures, *Vibration suppression of laminated shell structures investigated using higher order shear deformation theory* 1 (2004) 131176–131194.

[8] J.N. Reddy, A simple higher-order theory for laminated composite plates, *ASME Journal of applied mechanics* (1984) 51745–51752.

[9] J.N. Reddy, C.F. Liu, A higher-order shear deformation theory for laminated elastic shells, *International Journal of Engineering Science* (1985) 23319–23330.

[10] G. Maidanik, Response of ribbed panels to a reverberant acoustic fields, *Journal of the Acoustical Society of America* (1962) 34809–34826.

[11] G. Maidanik, Surface-Impedance nonuniformities as wave-vector convectors, *Journal of the Acoustical Society of America* (1969) 461062–461073.

[12] D.G. Crighton, G. Maidanik, Acoustic and vibration fields generated by ribs and fluid-loaded panel I: Plane wave problems for a single rib, *Journal of sound and vibration* (1981) 75437–75452.

[13] B.R. Mace, Sound radiation form a plate reinforced by two sets of parallel stiffeners, *Journal of Sound and Vibration* 71 (3) (1980) 435–441.

[14] D.J. Mead, K.K. Pujara, Spacing harmonic analysis of periodically supported beams: response to convected random loading, *Jounral of sound and vibration* (1971) 14525–14541.

[15] D.J. Mead, Y. Yaman, The harmonic response of rectangular sandwich plates with multiple stiffening: a flexural wave analysis, *HJournal of Sound and Vibration* 145 (3) (1991) 409–428.

[16] C.B. Burroughs, Acoustic radiation from fluid-loaded infinite circular cylinders with doubly periodic supports, *Journal of the Acoustical Society of America* 75 (3) (1984) 715–722.

[17] M.L. Rumerman, Vibration and wave propagation in ribbed plates, *Journal of the Acoustical Society of America* 57 (2) (1975) 370–373.

[18] R.F. Keltie, Structural acoustic response of finite rib-reinforced plates, *Journal of the Acoustical Society of America* 94 (2) (1993) 880–887.

[19] Y.F. Hwang, M. Kim, P.J. Zoccola, Acoustic radiation by point- or line-excited laminated plates, *ASME Journal of vibration and acoustics* 122 (2000) 189–195.

[20] O. Foin, J. Nicolas, N. Atalla, An efficient tool for predicting the structural acoustic and vibration response of sandwich plates in light or heavy fluid, *HApplied Acoustics H* 57 (3) (1999) 213–242.

[21] J.N. Reddy, *Mechanics of laminated composite plates: theory and analysis*, CRC Press, Boca Raton, 1997.

[22] M.C. Junger, D. Feit, *Sound, Structure, and Their Interaction*, second ed, MIT Press, Cambridge, MA, 1986 (pp. 214–215).